Computers & Structures Vol. 32, No. 5, pp. 1125–1132, 1989
Printed in Great Britain.

0045-7949/89 \$3.00 + 0.00

A HIGHER-ORDER THEORY FOR FREE VIBRATION OF UNSYMMETRICALLY LAMINATED COMPOSITE AND SANDWICH PLATES—FINITE ELEMENT EVALUATIONS

T. Kant and Mallikarjuna
Department of Civil Engineering, Indian Institute of Technology, Powai, Bombay—400 076, India

(*Received* 25 *May* 1988)

Abstract—This paper presents a refined higher-order theory for free vibration analysis of unsymmetrically laminated multilayered plates. The theory accounts for parabolic distribution of the transverse shear strains through the thickness of the plate and rotary inertia effects. A simple C^0 finite element formulation is presented and the nine-noded Lagrangian element is chosen with seven degrees of freedom per node. Numerical results are presented showing the parametric effects of aspect ratio, length/thickness ratio, number of layers, and lamination angle. The present theory predicts the frequencies more accurately when compared with first-order and classical plate theories.

INTRODUCTION

With the increase in the usage of multilayered structures in the field of structural engineering, the search for various methods for studying the dynamic behaviour of these structures has gained momentum. A great variety of shear deformation theories have been proposed and some are reviewed in [1]. They range from the first such theory by Yang *et al.* [2] for laminated anisotropic plates to various effective stiffness theories such as those discussed by Sun and Whitney [3], Whitney and Sun's higher-order theory [4] and the three-dimensional elasticity theory approach of Srinivas *et al.* [5, 6] and Noor [7]. Fortier and Rossettos [8] analysed free vibration of thick rectangular plates of unsymmetric cross-ply construction, while Sinha and Rath [9] considered both vibration and buckling for the same type of plates. Bert and Chen [10] presented a closed form solution for free vibration of anti-symmetric angle-ply laminates using the theory of Yang *et al.* [2].

While considerable effort has been expended in the finite element vibration analysis of isotropic plates, only limited investigations of laminated anisotropic plates can be found in the literature [11, 12, 19]. In recent years, many refined plate theories have been presented to improve the static [13–16] and the dynamic [17–21] themes of laminated construction. The present paper attempts to provide a simple refined higher-order theory with a C^0 finite element formulation. With the simplicity of this model, economic solutions can be obtained for both symmetric and anti-symmetric multi-layered composite and sandwich plates. A special mass matrix diagonalization scheme is adopted which conserves the total mass of the element and includes the effects due to rotary inertia terms.

GOVERNING EQUATIONS

In this section, a brief presentation of the governing equations of motion corresponding to the present shear deformation theory is given. The matrix equation governing free vibrations may be expressed as

$$\mathbf{Kd} - \omega^2\mathbf{Md} = \mathbf{0}, \tag{1a}$$

where **K** and **M** are the global stiffness and mass matrices respectively (obtained by the assembly of the corresponding element matrices), **d** is the vector of global nodal displacements and ω is the natural frequency of free vibration of the system. For the purpose of evaluation, eqn (1a) is converted to the standard eigenvalue format,

$$(\mathbf{K} - \lambda\mathbf{M})\mathbf{d} = \mathbf{0} \quad \text{with } \lambda = \omega^2. \tag{1b}$$

A subspace iteration technique [23] is used to obtain the eigenvalues λ_i and the corresponding eigenvectors $\mathbf{d}_i$.

A Cartesian co-ordinate system (x, y, z) is considered. The total thickness of plate (h_1, h_2, h_3, etc., are the individual thicknesses in the case of a layered plate) is assumed to be h; a and b are assumed to be the length and width of the plate. The components of displacements are taken as follows (see Fig. 1):

$$u(x, y, z, t) = u_0(x, y, t) + z\psi_x(x, y, t) + z^3\psi_x^*(x, y, t)$$

$$v(x, y, z, t) = v_0(x, y, t) + z\psi_y(x, y, t) + z^3\psi_y^*(x, y, t)$$

$$w(x, y, z, t) = w_0(x, y, t). \tag{2}$$

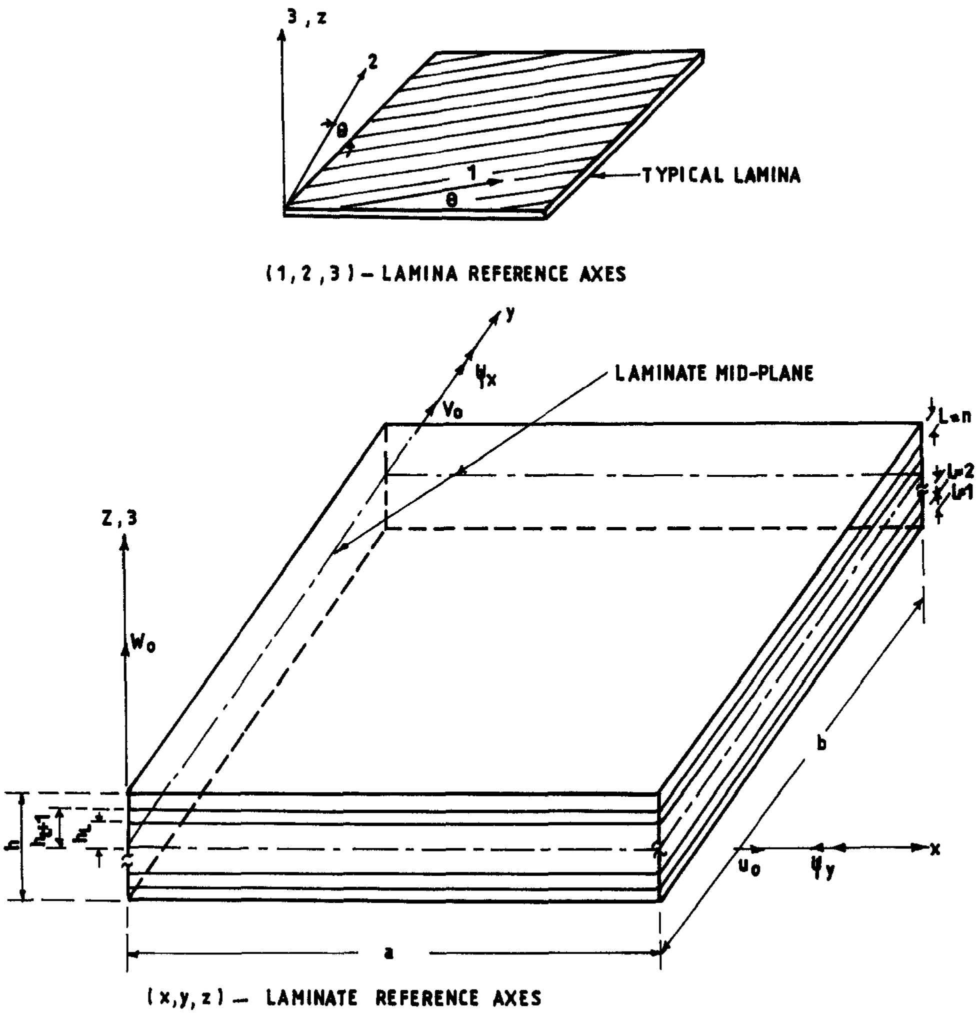

Fig. 1. Laminate geometry with positive set of lamina/laminate reference axes, displacement components and fibre orientation.

In these equations, u, v, w are the displacement components of a generic point in plate space in the x-, y-, z-directions, respectively; u_0, v_0 are the in-plane (stretching) displacements of a point lying in the middle plane, and ψ_x and ψ_y are the normal rotations about the y and x axes respectively. The higher-order terms ψ_x^* and ψ_y^* account for the flexural mode of deformation in the Taylor series expansion and are also defined at the midplane.

The strain–displacement relations, using the above displacement forms, may be written as

$$\epsilon_x = \frac{\partial u_0}{\partial x} + z\frac{\partial \psi_x}{\partial x} + z^3\frac{\partial \psi_x^*}{\partial x}$$

$$\epsilon_y = \frac{\partial v_0}{\partial y} + z\frac{\partial \psi_y}{\partial y} + z^3\frac{\partial \psi_y^*}{\partial y}$$

$$\epsilon_z = 0$$

$$\gamma_{xy} = \left(\frac{\partial u_0}{\partial y} + \frac{\partial v_0}{\partial x}\right) + z\left(\frac{\partial \psi_x}{\partial y} + \frac{\partial \psi_y}{\partial x}\right) + z^3\left(\frac{\partial \psi_x^*}{\partial y} + \frac{\partial \psi_y^*}{\partial x}\right)$$

$$\gamma_{yz} = \left(\psi_y + \frac{\partial w_0}{\partial y}\right) + z^3(3\psi_y^*)$$

$$\gamma_{xz} = \left(\psi_x + \frac{\partial w_0}{\partial x}\right) + z^2(3\psi_x^*). \quad (3)$$

Owing to the existence of a plane of elastic symmetry, the constitutive relations for any layer in the (x, y) system are of the form

$$\sigma_x = Q_{11}\epsilon_x + Q_{12}\epsilon_y + Q_{13}\gamma_{xy}$$

$$\sigma_y = Q_{12}\epsilon_x + Q_{22}\epsilon_y + Q_{23}\gamma_{xy}$$

$$\tau_{xy} = Q_{13}\epsilon_x + Q_{23}\epsilon_y + Q_{33}\gamma_{xy}$$

$$\tau_{yz} = Q_{44}\gamma_{yz} + Q_{45}\gamma_{zx}$$

$$\tau_{zx} = Q_{45}\gamma_{yz} + Q_{55}\gamma_{zx}, \quad (4a)$$

where

$$Q_{11} = C_{11}c^4 + 2(C_{12} + 2C_{33})s^2c^2 + C_{22}s^4$$

$$Q_{12} = (C_{11} + C_{22} - 4C_{33})s^2c^2 + C_{12}(s^4 + c^4)$$

$$Q_{22} = C_{11}s^4 + 2(C_{12} + 2C_{33})s^2c^2 + C_{22}c^4$$

$$Q_{13} = (C_{11} - C_{12} - 2C_{66})sc^3 + (C_{12} - C_{22} + 2C_{66})s^3c$$

$$Q_{23} = (C_{11} - C_{12} - 2C_{33})s^3c + (C_{12} - C_{22} + 2C_{33})sc^3$$

$$Q_{33} = (C_{11} + C_{22} - 2C_{12} - 2C_{33})s^2c^2 + C_{66}(s^4 + c^4)$$

$$Q_{44} = C_{44}c^2 + C_{55}s^2$$

$$Q_{45} = (C_{55} - C_{44})sc$$

$$Q_{55} = C_{44}s^2 + C_{55}c^2, \tag{4b}$$

in which

$$C_{11} = \frac{E_1}{1 - \nu_{12}\nu_{21}}; \quad C_{12} = \frac{\nu_{12}E_2}{1 - \nu_{12}\nu_{21}}; \quad C_{22} = \frac{E_2}{1 - \nu_{12}\nu_{21}};$$

$$C_{33} = G_{12}; \quad C_{44} = G_{23}; \quad C_{55} = G_{13}. \tag{4c}$$

We have the following definitions for stress-resultant expressions appropriate to the present shear deformation theory:

$$\begin{bmatrix} N_x, & M_x, & M_x^* \\ N_y, & M_y, & M_y^* \\ N_{xy}, & M_{xy}, & M_{xy}^* \end{bmatrix} = \sum_{L=1}^{n} \int_{h_L}^{h_{L+1}} \begin{bmatrix} \sigma_x \\ \sigma_y \\ \tau_{xy} \end{bmatrix} (1, z, z^3)\,\mathrm{d}z \tag{5a}$$

$$\begin{bmatrix} Q_x, & Q_x^* \\ Q_y, & Q_y^* \end{bmatrix} = \sum_{L=1}^{n} \int_{h_L}^{h_{L+1}} \begin{bmatrix} \tau_{xz} \\ \tau_{yz} \end{bmatrix} (1, z^2)\,\mathrm{d}z. \tag{5b}$$

Substituting eqns (4) in eqns (5) and integrating with respect to z we obtain the stress-resultants expressed in terms of seven generalized displacements as

$$\bar{\sigma} = \mathbf{D}\bar{\epsilon} \tag{6a}$$

$$\begin{bmatrix} N_x \\ N_y \\ N_{xy} \\ M_x \\ M_y \\ M_{xy} \\ M_x^* \\ M_y^* \\ M_{xy}^* \end{bmatrix} = \sum_{L=1}^{n} \begin{bmatrix} Q_{11}H_1 & Q_{22}H_1 & Q_{13}H_1 & Q_{11}H_2 & Q_{12}H_2 & Q_{13}H_2 & Q_{11}H_4 & Q_{12}H_4 & Q_{13}H_4 \\ & Q_{22}H_1 & Q_{23}H_1 & Q_{12}H_2 & Q_{22}H_2 & Q_{23}H_2 & Q_{12}H_4 & Q_{22}H_4 & Q_{23}H_4 \\ & & Q_{33}H_1 & Q_{13}H_2 & Q_{23}H_2 & Q_{33}H_2 & Q_{13}H_4 & Q_{23}H_4 & Q_{33}H_4 \\ & & & Q_{11}H_3 & Q_{12}H_3 & Q_{13}H_3 & Q_{11}H_5 & Q_{12}H_5 & Q_{13}H_5 \\ & & & & Q_{22}H_3 & Q_{23}H_3 & Q_{12}H_5 & Q_{22}H_5 & Q_{23}H_5 \\ & \text{SYMMETRIC} & & & & Q_{33}H_3 & Q_{13}H_5 & Q_{23}H_5 & Q_{33}H_5 \\ & & & & & & Q_{11}H_7 & Q_{12}H_7 & Q_{13}H_7 \\ & & & & & & & Q_{22}H_7 & Q_{23}H_7 \\ & & & & & & & & Q_{33}H_7 \end{bmatrix} \begin{bmatrix} \frac{\partial u_0}{\partial y} \\ \frac{\partial v_0}{\partial y} \\ \frac{\partial u_0}{\partial y} + \frac{\partial v_0}{\partial x} \\ \frac{\partial \psi_x}{\partial x} \\ \frac{\partial \psi_y}{\partial y} \\ \frac{\partial \psi_x}{\partial y} + \frac{\partial \psi_y}{\partial x} \\ \frac{\partial \psi_x^*}{\partial x} \\ \frac{\partial \psi_y^*}{\partial y} \\ \frac{\partial \psi_x^*}{\partial y} + \frac{\partial \psi_y^*}{\partial x} \end{bmatrix} \tag{6b}$$

$$\begin{bmatrix} Q_x \\ Q_y \\ Q_x^* \\ Q_y^* \end{bmatrix} = \sum_{L=1}^{n} \begin{bmatrix} Q_{55}H_1 & Q_{54}H_1 & Q_{55}H_3 & Q_{54}H_3 \\ & Q_{44}H_1 & Q_{45}H_3 & Q_{44}H_3 \\ & & Q_{55}H_5 & Q_{45}H_5 \\ \text{SYMMETRIC} & & & Q_{44}H_5 \end{bmatrix} \begin{bmatrix} \psi_x + \partial w_0/\partial x \\ \psi_y + \partial w_0/\partial y \\ 3\psi_x^* \\ 3\psi_y^* \end{bmatrix}. \tag{6c}$$

In the above relations, η is the number of layers and

$$H_i = \frac{1}{i}\,(h^i_{L+1} - h^i_L),\ i = 1, 2, 3, 4, 5, 7. \qquad (6d)$$

ELEMENT STIFFNESS MATRIX

In the present paper, the element under consideration is a nine-noded Lagrangian quadrilateral isoparametric element. At any point, the continuum displacement vector within the element is discretized such that

$$\boldsymbol{\delta} = \sum_{i=1}^{NN} N_i \boldsymbol{\delta}_i, \qquad (7a)$$

where N_i is the shape function associated with node i, NN is the number of nodes in an element, and

$$\boldsymbol{\delta}_i = [u_{oi}, v_{oi}, w_{oi}, \psi_{xi}, \psi_{yi}, \psi^*_{xi}, \psi^*_{yi}]^T. \qquad (7b)$$

The generalized strain $\bar{\boldsymbol{\varepsilon}}$ at any point within an element can be expressed by the following relationship:

$$\bar{\boldsymbol{\varepsilon}} = \sum_{i=1}^{NN} \mathbf{B}_i \boldsymbol{\delta}_i, \qquad (8a)$$

where

$$\bar{\boldsymbol{\varepsilon}} = \left[\frac{\partial u_0}{\partial x}, \frac{\partial v_0}{\partial y}, \frac{\partial u_0}{\partial y} + \frac{\partial v_0}{\partial x}, \frac{\partial \psi_x}{\partial x}, \frac{\partial \psi_y}{\partial y}, \frac{\partial \psi_x}{\partial y} + \frac{\partial \psi_y}{\partial x}, \frac{\partial \psi^*_x}{\partial x}, \frac{\partial \psi^*_y}{\partial y}, \frac{\partial \psi^*_x}{\partial y} + \frac{\partial \psi^*_y}{\partial x}, \psi_x + \frac{\partial w_o}{\partial x}, \psi_y + \frac{\partial w_o}{\partial y}, 3\psi^*_x, 3\psi^*_y\right]^T. \qquad (8b)$$

Elements of non-zero terms of strain–displacement matrix $\mathbf{B}$ are given below:

$$B_{1,1} = B_{3,2} = B_{4,4} = B_{6,5} = B_{7,6} = B_{9,7} = B_{10,3} = \frac{\partial N_i}{\partial x}$$

$$B_{10,4} = B_{11,5} = N_i$$

$$B_{2,2} = B_{3,1} = B_{5,5} = B_{6,4} = B_{8,7}, B_{9,6} = B_{11,3} = \frac{\partial N_i}{\partial y}$$

$$B_{12,6} = B_{13,7} = 3N_i. \qquad (8c)$$

Upon evaluating the $\mathbf{D}$ and $\mathbf{B}_i$ matrices as given by eqns (6) and (8) respectively, the element stiffness matrix can be readily computed using the standard relation

$$\mathbf{K}^e_{ij} = \int_{-1}^{1}\int_{-1}^{1} \mathbf{B}_i^T \mathbf{D} \mathbf{B}_j |\mathbf{J}|\, d\xi\, d\eta, \qquad (9)$$

where $\mathbf{J}$ is the Jacobian matrix.

ELEMENT MASS MATRIX

A diagonal mass matrix is more sophisticated than a lumped mass matrix as used here. It is derived from a consistent mass matrix and is discussed elsewhere [20–22].

The mass $\mathbf{M}$ in eqn (1) is given by

$$\mathbf{M} = \int_A \mathbf{N}^T \mathbf{m} \mathbf{N}\, d(\text{Area}), \qquad (10a)$$

where

$$\mathbf{N} = [N_1, N_2, N_3, \ldots, N_{NN}], \qquad (10b)$$

$$\mathbf{m} = \begin{bmatrix} I_1 & & & & & & \\ & I_1 & & & 0 & & \\ & & I_1 & & & & \\ & & & I_2 & & & \\ & 0 & & & I_2 & & \\ & & & & & I_3 & \\ & & & & & & I_3 \end{bmatrix} \qquad (10c)$$

in which

$$(I_1, I_2, I_3) = \sum_{L=1}^{n} \int_{h_L}^{h_{L+1}} (1, z^2, z^6)\rho^L\, dz,$$

where ρ^L is the material density of the Lth layer; I_1, I_2 and I_3 are normal inertia, rotary inertia and higher-order inertia terms respectively.

NUMERICAL EXAMPLES AND DISCUSSIONS

For the numerical computations, two computer programs were developed: PHOST7—Program for Higher Order Shear deformation Theory, with seven degrees of freedom per node; and PFOST5—Program for First Order Shear deformation Theory, with five degrees of freedom per node (i.e. Mindlin–Reissner theory). The selective integration scheme based on Gauss–quadrature rules, viz. 3×3 for membrane, coupling, flexure and inertia terms and 2×2 for shear terms, was employed. For all the numerical examples, a full plate is discretized with 4×4 mesh of the nine-noded Lagrangian quadrilateral elements. All the computations were carried out on CYBER 180/840 computer in single precision. The following material properties are used in the examples.

Material 1: Dimensionless material property (typical of graphite/epoxy)

$$\frac{E_1}{E_2} = 40, \quad \frac{G_{12}}{E_2} = \frac{G_{13}}{E_2} = 0.6, \quad \frac{G_{23}}{E_2} = 0.5, \quad \nu_{12} = 0.25.$$

The values of E_2 and ρ are arbitrary because of the non-dimensionalization used (set to unity here).

Material 2: Face-sheets (graphite/epoxy prepreg system):

$$E_1 = 1.308 \times 10^7 \text{ N/cm}^2, \quad E_2 = 1.06 \times 10^6 \text{ N/cm}^2$$

$$G_{12} = G_{13} = 6.0 \times 10^5 \text{ N/cm}^2, \quad G_{23} = 3.9 \times 10^5 \text{ N/cm}^2$$

$$\rho = 1.58 \times 10^{-5} \text{ N-sec}^2/\text{cm}^4, \quad \nu_{12} = 0.28$$

thickness of each top stiff layer $= 0.025h$
thickness of each bottom stiff layer $= 0.01825\,h$.

Core (U.S. commercial aluminium honeycomb 1/4-inch cell size, 0.003-in. foil):

$$G_{23} = 1.772 \times 10^4 \text{ N/cm}^2, \quad G_{13} = 5.206 \times 10^4 \text{ N/cm}^2$$

$$\rho = 1.009 \times 10^{-6} \text{ N-sec}^2/\text{cm}^4$$

thickness of core $= 0.6\,h$.

The boundary conditions used for the simply supported and clamped plates are as follows:

1. (a) Cross-ply boundary conditions (WSS1)

$$v_0 = w_0 = \theta_y = \theta_y^* = 0 \quad \text{at } x = 0, a$$

$$u_0 = w_0 = \theta_x = \theta_x^* = 0 \quad \text{at } y = 0, b.$$

(b) Angle-ply boundary conditions (WSS2)

$$u_0 = w_0 = \theta_y = \theta_y^* = 0 \quad \text{at } x = 0, a$$

$$v_0 = w_0 = \theta_x = \theta_x^* = 0 \quad \text{at } y = 0, b.$$

2. Clamped plate (WCC)

$$u_0 = v_0 = w_0 = \theta_x = \theta_y = \theta_x^* = \theta_y^* = 0 \text{ on all edges.}$$

The results presented in Tables 1–4 pertain to material 1. The effects of orthotropy, number of layers and the coupling between bending and stretching of the skew–symmetric laminate on the fundamental frequencies are shown in Table 1. The ratio of E_1/E_2 was varied between 3 and 40 and number of layers varied between two and 10. The predictions in Table 1 are compared with those obtained by 3D elasticity theory [7]. The present results are very close to 3D-elasticity solutions. It was also found that for skew–symmetrically laminated plates, as the number of layers increased from two to four, the accuracy of the CPT sharply deteriorated. Further increase of the number of layers does not have a significant effect on the accuracy. The error in the CPT predictions is mainly attributed to the neglect of shear deformation. This is demonstrated by the fact that the error in the predictions of present theory did not exceed 2.5% (even for the case of a highly orthotropic thick plate with $E_1/E_2 = 40$, $a/h = 5$). It is seen that the fundamental frequency increases with the increase in number of layers and/or increase of degree of orthotropy.

Two problems are further considered with material 1: (1) a two-layer, equal thickness, antisymmetric angle-ply (45°/ − 45°) square plate, (2) an eight-layer, equal thickness, antisymmetric angle-ply (45°/ − 45°/45° . . .) square plate. The smallest circular frequencies as a function of plate side-to-thickness ratios are tabulated in Table 2. The CPT solution is obtained with the rotary inertia terms included. It is found that the results of the present higher-order

Table 1. Effect of degree of orthotropy of individual layers on the fundamental frequency of simply supported square multilayered composite plates with $a/h = 5$; $\bar{\omega} = \omega(\rho h^2/E_2)^{1/2}$, material 1 (WSS1)

Source	No. of layers	E_1/E_2 = 3	10	20	30	40
3D elasticity theory [7]	2	0.25031	0.27938	0.30698	0.32705	0.34250
Present		0.24909	0.27981	0.31252	0.33414	0.35138
		(−0.48)	(+0.15)	(+1.80)	(+2.16)	(+2.59)
CPT		0.27082	0.30968	0.35422	0.39335	0.42884
		(+8.19)	(+10.84)	(+15.38)	(+20.27)	(+25.21)
3D elasticity theory [7]	4	0.26182	0.32578	0.37622	0.40660	0.42719
Present		0.26055	0.32870	0.38014	0.41247	0.43786
		(−0.48)	(+0.89)	(+1.04)	(+1.44)	(+2.49)
CPT		0.28676	0.38877	0.49907	0.58900	0.66690
		(+9.52)	(19.33)	(+32.65)	(+44.86)	(+56.11)
3D elasticity theory [7]	6	0.26440	0.33657	0.39359	0.42783	0.45091
Present		0.26275	0.33712	0.39784	0.43526	0.46090
		(−0.62)	(+1.16)	(+1.07)	(+1.73)	(+2.21)
CPT		0.28966	0.40215	0.52234	0.61963	0.70359
		(+9.55)	(+19.48)	(+32.71)	(+44.83)	(+56.03)
3D elasticity theory [7]	10	0.26583	0.34250	0.40337	0.44011	0.46498
Present		0.26389	0.34142	0.40377	0.44178	0.46771
		(−0.72)	(−0.31)	(+0.09)	(+0.37)	(+0.58)
CPT		0.29115	0.40888	0.53397	0.63489	0.72184
		(+9.52)	(+19.38)	(+32.37)	(+44.25)	(+55.24)

Values in parenthesis give percentage errors with respect to the elasticity solution [7].

Table 2. Non-dimensionalized fundamental frequencies, $\bar{\omega} = (\omega a^2/h)\sqrt{(\rho/E_2)}$ of simply supported anti-symmetric angle-ply square plates (WSS2), material 1

	[45/−45]			[45/−45/............] 8-layer		
a/h	Present HOST	Closed form solution [17]	CPT	Present HOST	Closed form solution [17]	CPT
5	10.692 (−1.36)	10.840	13.885 (+28.09)	12.967 (−0.038)	12.972	15.708 (+21.09)
10	13.207 (−0.42)	13.263	14.439 (+8.86)	19.274 (−0.041)	19.266	25.052 (30.03)
20	14.228 (−0.12)	14.246	14.587 (+2.39)	23.236 (−0.012)	23.239	25.212 (+8.49)
50	14.568 (−0.027)	14.572	14.630 (+0.39)	24.901 (−0.016)	24.905	25.258 (+1.41)
100	14.619 (−0.013)	14.621	14.636 (+0.102)	25.173 (−0.004)	25.174	25.264 (+0.35)

Values in brackets give percentage errors with respect to the closed form solution [17].

Table 3. Dimensionless fundamental frequencies, $\bar{\omega} = \omega a^2(\rho/E_2h^2)^{1/2}$, for various longitudinal and transverse wave numbers (m and n) of a simply supported square plate; $a/h = 10$, material 1 stacking sequence: 45/−45/45/−45, WSS2

					Reddy [12]			
m	n	Present HOST	Present FOST	Bert and Chen [10]	Half-plate 2 × 2 $NDF = 5$	Half-plate 2 × 2 $NDF = 3$	Half-plate 4 × 2 $NDF = 3$	Classical plate theory
1	1	18.32	18.45	18.46	18.259	19.244	19.153	23.53
1	2	34.54	34.54	34.87	35.585	36.512	35.405	53.74
2	2	49.71	49.99	50.52	—	—	—	94.11
1	3	53.63	53.87	54.27	54.367	55.727	55.390	98.87
2	3	65.02	65.08	67.17	70.315	70.895	67.637	147.65
1	4	75.65	75.25	75.28	79.315	79.882	76.412	160.35
3	3	83.14	81.99	82.84	99.597	100.012	84.725	211.75
2	4	86.75	85.05	85.27	—	—	—	214.97
1	5	99.45	98.46	97.56	108.665	109.792	105.057	238.72
3	4	100.88	99.45	99.02	—	182.255	109.292	288.76
2	5	103.28	100.22	104.95	—	226.432	116.385	297.30

shear–deformation theory (HOST) are in excellent agreement with the closed form solution (CFS) [17]. It is obvious that the CPT overestimates the frequencies.

A comparison of the effects of both the longitudinal and transverse wave numbers (m and n) on the associated frequencies, as predicted by the present HOST and FOST with the CFS [10] and finite element results using FOST [12] and CPT, is made in Table 3. Just as in the cases of isotropic plates and cross-ply plates [24], it is seen that the difference between the predictions of the present theories (HOST and FOST) and CPT increases with increasing m and n. Results of the present HOST and FOST are very close to CFS [10], whereas FOST finite element results using an eight-noded serendipity element given by Reddy [12] are far away from the CFS [10]. This could be due to analysing angle-ply laminate by discretizing quarter- and/or half-plates. It should be noted that no mirror image of the cross-sectional plane of symmetry exists for angle-ply laminates and thus a full plate should be discretized for the analysis.

To facilitate extrapolation to aspect ratio (a/b) other than one or infinity, Table 4 presents dimensionless frequency as a function of a/b for various values of a/h and lamination angle. It is observed from the table that the fundamental frequencies decrease with the increase in lamination angle for $a/b = 0.5$, and for $a/b = 2.0$ frequencies increase with the increase in the lamination angle. As the a/h ratio increases, the fundamental frequency decreases.

Table 4. Effects of plate aspect ratio (a/b), lamination angle and length-to-thickness ratio (a/h) on the dimensionless fundamental frequency, $\bar{\omega} = \omega\ (\rho h^2/E_2)^{1/2} \times 10$, of a simply supported rectangular plate (material 1) of stacking sequence ($\theta/-\theta/\theta/-\theta$)

		a/b			
$\frac{a}{h}$	$\theta°$	0.5	1.0	2.0	4.0
5	30	3.7448	4.8554	7.5261	15.3144
	45	3.4594	5.0178	8.5404	17.0529
	60	2.9357	4.8554	8.9875	11.6581
10	30	1.2829	1.7513	2.9357	6.1819
	45	1.1501	1.8326	3.4594	7.5371
	60	0.9376	1.7513	3.7448	5.9289
20	30	0.3646	0.5165	0.9376	2.1461
	45	0.3213	0.5450	1.1501	2.8785
	60	0.2563	0.5165	1.2829	2.9793
50	30	0.0609	0.0877	0.1660	0.4121
	45	0.0533	0.0928	0.2088	0.5962
	60	0.0422	0.0877	0.2376	0.7621

Table 5. Comparison of natural frequencies ($\omega/2\pi$) of an eight-layer (0/45/90/core/90/45/30/0) square composite-sandwich plate (material 2, $a = b = 100$ cm)

Modal nos.	Considering G_{23} and G_{13} of stiff layers								Neglecting G_{23} and G_{13} of stiff layers							
	Simply supported (WSS2)				Clamped (WCC)				Simply supported (WSS2)				Clamped (WCC)			
	$a/h = 10$		$a/h = 100$		$a/h = 10$		$a/h = 100$		$a/h = 10$		$a/h = 100$		$a/h = 10$		$a/h = 100$	
	HOST	FOST	HOST	FOST	HOST	FOST	HOST	FOST	HOST	FOST	HOST	FOST	HOST	FOST	HOST	FOST
1	485	516	59	59	686	754	102	102	305	297	58	58	341	332	98	98
2	926	1013	127	127	1093	1244	192	192	452	430	123	123	470	446	177	176
3	1063	1154	154	154	1238	1382	231	231	580	579	150	150	607	586	216	216
4	1355	1501	210	211	1508	1706	295	296	619	582	202	201	628	595	269	268
5	1531	1773	265	265	1664	1961	375	378	673	656	246	243	691	666	320	314
6	1747	1993	321	322	1825	2150	440	444	731	673	299	297	735	674	380	374
7	1781	2042	326	327	1916	2173	459	462	737	678	309	309	737	680	411	411
8	1791	2173	387	389	1921	2222	526	531	780	744	359	357	792	750	445	432

In the last example, thick and thin composite-sandwich plates (material 2) were analysed using present HOST and FOST for two different boundary conditions: simply supported and clamped. It is seen from Table 5 that for a thick plate ($a/h = 10$), the difference between the predictions of the two theories (HOST and FOST) increases with increasing mode numbers. The effect of shear modulii G_{23} and G_{13} of stiff layers are more pronounced in thicker plates than for thin plates.

CONCLUSION

A refined higher-order theory with simple C^0 finite element formulation for the vibration of anisotropic laminates is presented. This model can take into account any lamina material properties. The predictions of anisotropic laminated plate behaviour are in good agreement with 3D elasticity solutions and closed form solutions of a higher-order theory. The effects of plate aspect ratio on the fundamental frequencies and transverse shear moduli of stiff layers on the natural frequencies are more pronounced in thicker plates than in thin plates. The errors in CPT and FOST as compared with HOST increase very severely with an increase in either the longitudinal or the transverse wave numbers. The present theory does not require any shear correction coefficients and the results reaffirm that the effects of anisotropy, transverse shear deformation, thickness and plate aspect ratio play an important role in the free vibration frequencies of anisotropic laminates.

REFERENCES

1. C. W. Bert, Analysis of plates. In *Structural Design and Analysis*, Part I (Edited by C. C. Chamis), Chapter 4, p. 149. Academic Press, New York (1974).
2. P. C. Yang, C. H. Norris and Y. Stavsky, Elastic wave propagation in heterogeneous plates. *Int. J. Solids Struct.* **2**, 665–684 (1966).
3. C. T. Sun and J. M. Whitney, Theories for the dynamic response of laminated plates. *AIAA J.* **11**, 178–183 (1973).
4. J. M. Whitney and C. T. Sun, A higher order theory for extensional motion of laminated composites. *J. Sound Vibrat.* **30**, 85–97 (1973).
5. S. Srinivas and A. K. Rao, Bending, vibration and buckling of simply supported thick orthotropic rectangular plates and laminates. *Int. J. Solids Struct.* **6**, 1463–1481 (1970).
6. S. Srinivas, C. V. Joga Rao and A. K. Rao, An exact analysis for vibration of simply supported homogeneous and laminated thick rectangular plates. *J. Sound Vibrat.* **12**, 187–199 (1970).
7. A. K. Noor, Free vibrations of multilayered composite plates. *AIAA J.* **11**, 1938–1939 (1973).
8. R. C. Fortier and J. N. Rossettos, On the vibration of shear deformable curved anisotropic composite plates. *J. appl. Mech.* **40**, 299–301 (1973).
9. P. K. Sinha and A. K. Rath, Vibration and buckling of cross-ply laminated circular cylindrical panels. *Aeronaut. Q.* **26**, 211–218 (1975).
10. C. W. Bert and T. L. C. Chen, Effect of shear deformation on vibration of antisymmetric angle-ply laminated

rectangular plates. *Int. J. Solids Struct.* **14**, 465–473 (1978).
11. E. Hinton, A note on a finite element method for the free vibrations of laminated plates (short communication). *Earthquake Engng Struct. Dyn.* **4**, 515–516 (1976).
12. J. N. Reddy, Free vibration of antisymmetric, angle-ply laminated plates including transverse shear deformation by the finite element method. *J. Sound Vibrat.* **4**, 565–576 (1979).
13. T. Kant, Numerical analysis of thick plates. *Comput. Meth. appl. Mech. Engng* **31**, 1–18 (1982).
14. T. Kant, D. R. J. Owen and O. C. Zienkiewicz, A refined higher-order C^0 plate bending element. *Comput. Struct.* **15**, 177–183 (1982).
15. B. N. Pandya and T. Kant, Flexural analysis of laminated composites using refined higher-order C^0 plate bending elements. *Comput. Meth. appl. Mech. Engng* **66**, 173–198 (1988).
16. B. N. Pandya and T. Kant, A refined higher-order generally orthotropic C^0 plate bending element. *Comput. Struct.* **28**, 119–133 (1988).
17. J. N. Reddy and N. D. Phan, Stability and vibration of isotropic and laminated plates according to a higher-order shear deformation theory. *J. Sound Vibrat.* **98**, 157–170 (1985).
18. N. S. Putch and J. N. Reddy, Stablity and vibration analysis of laminated plates by using a mixed element based on a refined plate theory. *J. Sound Vibrat.* **104**, 285–300 (1986).
19. D. R. J. Owen and Z. H. Li, A refined analysis of laminated plates by finite-element displacement methods—II. Vibration and stability. *Comput. Struct.* **26**, 915–923 (1987).
20. Mallikarjuna and T. Kant, Dynamics of laminated composite plates with a higher-order theory and finite element discretization. *J. Sound Vibrat.* **126**, 463–475 (1988).
21. Mallikarjuna and T. Kant, Finite element formulation of a higher-order theory for dynamic response of laminated composite plates (under review).
22. E. Hinton, T. Rock and O. C. Zienkiewicz, A note on mass lumping and related processes in the finite element method. *Earthquake Engng Struct. Dyn.* **4**, 245–249 (1976).
23. K. J. Bathe, *Finite Element Procedures in Engineering Analysis*. Prentice-Hall, Englewood Cliffs, NJ (1982).
24. C. I. Wu and J. R. Vinson, The natural vibrations of plates composed of composite materials. *Fibre Sci. Technol.* **2**, 97 (1969).